# 3 Variable-pressure luminescence and Raman spectroscopy of molecular transition metal complexes: spectroscopic effects originating from small, reversible structural variations

**Christian Reber,*[a] Camille Sonneville,[a] Stéphanie Poirier,[a] Nicolas Bélanger-Desmarais,[a] William B. Connick,[b] Sayandev Chatterjee,[b] Patrick Franz,[c] Silvio Decurtins[c]**

**DOI: 10.1039/b000000x [DO NOT ALTER/DELETE THIS TEXT]**

The past ten years have seen a significantly increasing number of published crystal structures for molecular transition metal complexes at variable pressure, providing quantitative information on structural variations. Spectroscopic measurements at variable pressure have been reported over the past 60 years for a variety of complexes, but luminescence measurements were mostly limited to intense signals until early in this century. The combination of variable-pressure structure variations with spectroscopic trends can lead to detailed new insight on a variety of aspects of electronic structure. This approach holds promise for the in-depth study of many categories of functional materials.

## 1 Introduction

Vibrational and electronic spectroscopic techniques have been traditionally used as experimental probes for specific functional groups or symmetry aspects, i.e. as indirect techniques to determine partial structures. This is well illustrated by the title and a historical perspective in the introduction of the recent new edition of the graduate-level textbook "Structural Methods in Molecular Inorganic Chemistry" by Rankin, Mitzel and Morrison,[1] discussing many spectroscopic techniques as well as diffraction methods. In the following, we present a number of examples where the spectroscopic study goes beyond this traditional perspective toward an approach based on both structural data and spectroscopic information, leading to possibilities to correlate quantitative variations of spectroscopic properties with structure. External pressure applied to solids leads to structure modifications[2,3] and often to very significant spectroscopic effects.[4-7] Examples presented in the following overview are limited to reversible phenomena showing the spectroscopic effects resulting from structure changes at pressures below 10 GPa, a range easily accessible through standard diamond anvil cells.

Spectroscopic measurements under variable conditions have a long history, with variable-temperature studies[8,9] being more abundant than variable-pressure spectra. Fig. 1 shows an example of variable-temperature effects in the polarized absorption spectra of $[Nb^{IV}\{(\mu\text{-}CN)_4Mn^{II}(H_2O)_2\}_2{\cdot}4H_2O]_n$, a high-symmetry three-dimensional network with interesting magnetic properties that have been studied both at variable temperature and pressure.[10] As temperature increases, a broad, completely polarized band appears between 16000 and 16500 $cm^{-1}$. This "hot band" becomes intense at

temperatures above 100 K, whereas the magnetic properties change in a much lower temperature range. Its integrated intensity is given in the inset to Fig. 1 and shows a behavior typical for a thermal activation barrier of approximately 150 $cm^{-1}$, the order of magnitude of low-frequency metal-ligand vibrational modes. This is a typical signature for a vibronic intensity mechanism and the observed new "hot band" is not due to structural changes as temperature increases, but arises from varying populations of vibrational levels. Such effects make the analysis of spectroscopic changes due to temperature-dependent structure variations highly challenging if not impossible, an intrinsic problem of variable-temperature spectroscopic measurements.

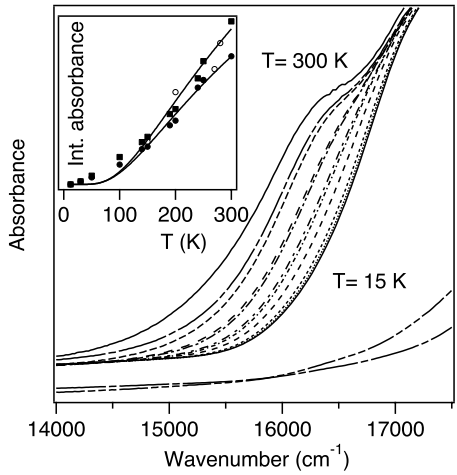


**Fig. 1** Temperature-dependent, polarized absorption spectra of $[Nb^{IV}\{(\mu\text{-}CN)_4Mn^{II}(H_2O)_2\}_2{\cdot}4H_2O]_n$. Inset : integrated absorption intensity between 15000 $cm^{-1}$ and 16700 $cm^{-1}$ with solid traces calculated for activation energies of 150 $cm^{-1}$ and 200 $cm^{-1}$.

Variable-pressure measurements, often carried out at room temperature, do not have this problem. In general, structural changes induced by pressure do not lead to drastic changes of vibrational frequencies, and therefore thermal populations are constant and spectroscopic features are more easily analyzed in terms of structure variations. Until very recently, only a handful of variable-pressure structural studies had been published. As an example, a search in the Cambridge Structural Database published in 2006 lists 7 structures. Our literature search has revealed more than 30 structures published since 2006, as summarized in Table 1. This increase has been made possible by advances in X-ray diffraction equipment, from intense synchrotron sources to highly sensitive detectors and advanced computational tools. This very significant increase in available data is likely to continue, and the combination of structural and spectroscopic data promises to lead to significant new knowledge relevant to many areas of chemistry, in particular to inorganic functional materials, such as single-molecule magnets[11] where both the electronic structure of molecular units and their intermolecular interactions are of key importance to materials characteristics.

Table 1. Overview of published variable-pressure structural studies

| Metal | Compound [ref] | Max. Pressure (GPa) (# pressures) | Techniques (Year) |
|---|---|---|---|
| Li | $LiB(Im)_4$ (ZIF) [12] | 1.69 (5) | XRD, Nano-Indentation (2010) |
| Gd(III) | $[Gd(PhCOO)_3(DMF)]_n$ [13] | 5.01 (8) | XRD (2010) |
| Mn(II), Nb(IV) | $\{[Mn(pydz)(H_2O)_2][Mn(H_2O)_2][Nb(CN)_8]_3H_2O\}_n$ [14] | 1.8 (1) | XRD, Magnetism (2012) |
| Mn(III) | $[Mn(pyrol)_3tren]$ [15] | 1 (2) | XRD (2005) |
| Mn(II) | $[(CH_3)_4N][MnCl_3]$ [16] | 1.7 (5) | XRD, Magnetism (2006) |
| Mn(III) | $[Mn_6O_2(Et\text{-}sao)_6(O_2CPh(Me)_2)_2\text{-}(EtOH)_6$ [17] | 1.5 (3) | XRD, Magnetism (2008) |
| Mn(III) | $[Mn_6O_2(Et\text{-}sao)_6(O_2C\text{-}naphth)_2(EtOH)_4(H_2O)_2]$ [18] | 1.5 (3) | XRD, Magnetism (2009) |
| Mn(III)/ Mn(II) | $[Mn_3(Hcht)_2(bpy)_4](ClO_4)_3Et_2O_2MeCN$ [18] | 1.25 (3) | XRD, Magnetism (2009) |
| Mn(III)/ Mn(IV) | $[Mn_2O_2(bpy)_4](PF_6)_3\cdot 2CH_3CN\cdot 1H_2O$ [19] | 4.55 (5) | XRD, Magnetism (2010) |
| Mn(III)/ Mn(IV) | $[Mn_2O_2(bpy)_4](ClO_4)_3\cdot 3CH_3CN$ [19] | 2 (3) | XRD, Magnetism (2010) |
| Mn(III) | $[Mn_{12}O_{12}(O_2CCH_2tBu)_{16}(H_2O)_4]CH_2C_{12}MeNO_2$ [20] | 2.5 (2) | XRD, Magnetism (2010) |
| Fe(II) | $Fe(1,10\text{-}Phen)_3(NCS)_2$ [21] | 1 (1) | XRD (1993) |
| Fe(II) | $Fe(Btz)_3(NCS)_2$ [21] | 0.95 (1) | XRD (1993) |
| Fe(II) | $[Fe(bapbpy)(NCS)_2]$ [22] | 1.09 (2) | XRD, Raman (2011) |
| Fe(II) | $[Fe(dpp)_2(NCS)_2]\cdot$pyridine [23] | 2.48 (7) | XRD, Magnetism, Raman (2012) |
| Ru(0) | $Ru_3(CO)_{12}$ [24] | 8.14 (7) | XRD, Raman, IR (2004) |
| Co(0) | $[Co_2(CO)_6(PPh_3)_2]$ [25] | 4.4 (6) | XRD (2005) |
| Co(II) | $(4\text{-Chloropyridinium})_2[CoCl_4]$ [26] | 3.73 (9) | XRD (2008) |
| Co (II) | $(4\text{-Chloropyridinium})_2[CoBr_4]$ [26] | 2.92 (9) | XRD (2008) |
| Co(0) | $[Co_2(CO)_6(AsPh_3)_2]$ [27] | 4.1 (8) | XRD (2009) |
| Ni(II) | bis(3-fluoro-salicylaldoximato)Ni [28] | 5.4 (7) | XRD, Absorption (2012) |
| Ni(II) | bis(3-methoxy-salicylaldoximato)Ni [28] | 5.56 (7) | XRD, Absorption (2012) |
| Pd(II) | *cis*-$[PdCl_2(1,4,7\text{-trithiacyclononane})]$ [29] | 5.35 (6) | XRD (2006) |
| Pd(II) | $Cs_2[PdI_4]I_2$ [30] | 3.7 (12) | XRD (2006) |
| Pd(II) | $Cs_2[PdBr_4]I_2$ [30] | 2.18 (9) | XRD (2006) |
| Pd (II) | $Cs_2[PdCl_4]I_2$ [30] | 4.1 (16) | XRD (2006) |
| Cu(II) | $[Cu_2(OH)_2(H_2O)_2(tetramethylethylenediamine)_2](ClO_4)_2$ [31] | 2.5 (4) | XRD, Magnetism (2009) |
| Cu(II) | $[Cu_2(OH)_2(di\text{-}tbutylethylenediamine)_2](ClO_4)_2$ [31] | 0.9 (2) | XRD, Magnetism (2009) |
| Cu(II) | $[Cu_2(OH)_2(2,2'\text{-bipyridine})_2](BF_4)_2$ [31]} | 4.7 (9) | XRD, Magnetism (2009) |
| Cu(II) | $[Cu_2(OH)(citrate)(Guanidine)_2]^-$ [32] | 4.23 (4) | XRD (2009) |

| | | | |
|---|---|---|---|
| Cu(II) | $[GuH]_4[Cu_2(cit)_2]_2H_2O$ [33] | 2.2 (3) | XRD (10), Absorption |
| Cu(II) | $[Cu(L\text{-}Aspartate)(H_2O)_2](CuAspartate)$ [34] | 7.9 (8) | XRD (2012) |
| Cu(II) | $[Cu(CO_3)_2](CH_6N_3)_2$ [35] | 3.95 (3) | XRD (2012) |
| Cu(II) | $[CuF_2(H_2O)_2(pyz)]$ [36] | 3.3 (8) | XRD, Magnetism (2012) |
| Ag(I) | Ag 2-methylimidazolate [37] | 6.4 (8) | XRD, Piezoelectric response (2012) |
| Au | [Au(trimethylene tetrathiafulvalenedithiolate)$_2$] [38] | 10.7 (6) | XRD (2009) |
| Au(I) | $[(C_6F_5Au)_2(m\text{-}1,4\text{-}diisocyanobenzene)]$ [39] | 4.39 (7) | XRD, Luminescence (2013) |
| Zn(II) | $[Zn_2(C_3H_3N_2)_4]n$ (ZIF: $ZnIm_2$) [40] | 0.54 (4) | XRD (2009) |
| Zn(II) | Porous Zn(2-methylimidazolate)$_2$ (ZIF-8) [41] | 1.47 (6) | XRD (2009) |
| Zn(II) | $[Zn(Im)_2]$ (ZIF-4) [42] | 4.39 (6) | XRD (2011) |
| Zn(II) | $[NH_4][Zn(HCOO)_3]$ [43] | 0.94 (7) | XRD (2012), Nano-indentation |

One example of structural variations induced by pressure is shown in Fig. 2 for a square-planar nickel(II) complex, one of many $d^8$ compounds with this coordination geometry. The unit cell of the crystal decreases by more than 25% over the pressure range studied, which is a very significant decrease. In contrast, metal-ligand bond lengths show a much less obvious variation with pressure, also illustrated in Fig. 2. Similar small changes are observed for all intramolecular distances. Despite their small changes, spectroscopic effects are easily measured, as shown in the following. The pressure-induced volume decrease mainly causes intermolecular distances to decrease, as shown in Fig. 2, illustrating the potential of variable-pressure spectroscopy to probe intermolecular effects.

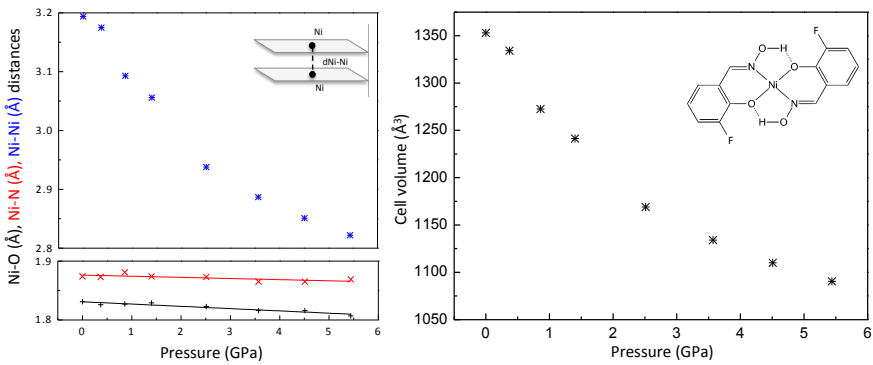


**Fig. 2** Variable-pressure unit cell volume of bis(3-fluorosalicylaldoximato)nickel(II) (right) and variable-pressure inter- and intramolecular distances: Ni-O (black), Ni-N (red) and $d_{Ni\text{-}Ni}$ (blue).

Fig. 3 schematically illustrates luminescence spectroscopic effects for square-planar transition metal compounds, a vast class of compounds similar to the example for which structural changes are shown in Fig. 2. Intramolecular effects on luminescence spectra can be qualitatively predicted from the bonding characteristics of the HOMO and LUMO levels: the σ* LUMO is destabilized very strongly by even the smallest bond length decrease, an effect that dominates the destabilization

of the π* HOMO levels in Fig. 3a. The result is an increase of the luminescence energy, leading to a shift of the maximum to higher energy or shorter wavelength, often denoted a blue shift in the literature. d-d transitions as illustrated in Fig. 3a have been investigated for many compounds, and shifts on the order of +10 $cm^{-1}$/kbar to +30 $cm^{-1}$/kbar are typical (shifts are given in $cm^{-1}$/kbar units throughout this report in order to be easily compared to the majority of published values, multiply by 10 to obtain $cm^{-1}$/GPa).[6,7] Intermolecular effects change the expected trend, also shown in Fig. 3a. They lead to an energy increase of the $d_{z2}$ level and therefore to a decrease of the HOMO-LUMO energy difference, a variation in the opposite direction of the trend derived from the intramolecular changes in Fig. 3a. From experimental spectra it is therefore straightforward to determine which effects dominate, but obviously the spectra do not give access to quantitative structural changes – the combination with diffraction data is essential. Fig. 3b represents other types of transitions, such as charge-transfer bands, with different variable-pressure properties than those in Fig. 3a. Fig. 3c shows an intermediate case, involving gold(I)-gold(I) interactions with distances that are easily shortened through the application of pressure, leading to very characteristic spectroscopic effects such as the strong decrease of the luminescence energy schematically illustrated in Fig. 3c. Experimental examples for these categories of phenomena will be presented in the following sections.

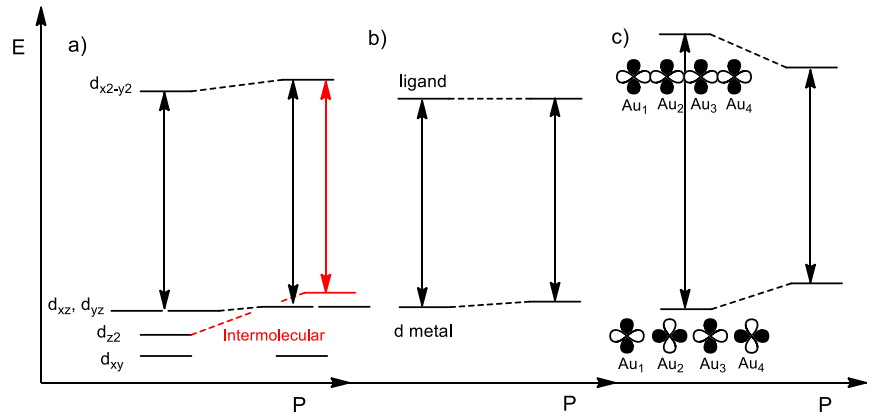


**Fig. 3** Schematic representation of pressure effects on HOMO and LUMO energies for typical d-d transitions in square-plan complexes (**a**), MLCT transition (**b**) and for a gold(I) dithiocarbamate polymer chain (**c**).

## 2 Structural changes and variable-pressure Raman spectroscopy

There is a rich literature on variable-pressure vibrational spectroscopy.[44,45] Changes in molecular vibrational frequencies are small in the pressure range of interest here, and not obvious to quantitatively correlate with small structural changes, such as those shown in Fig. 2. In contrast, structural phase transitions are revealed through characteristic discontinuous variations of frequencies, which makes this a very sensitive technique for detection of such changes. An illustrative class of compounds with intriguing changes of structures and properties in response to external stimuli are spin-crossover materials.[46] A recent perspective on these materials emphasizes

the importance of combining an array of techniques and conditions such as variable pressure and temperature. Very significant shifts of vibrational frequencies occur as a consequence of the spin transition and its changes in metal-ligand bonding.

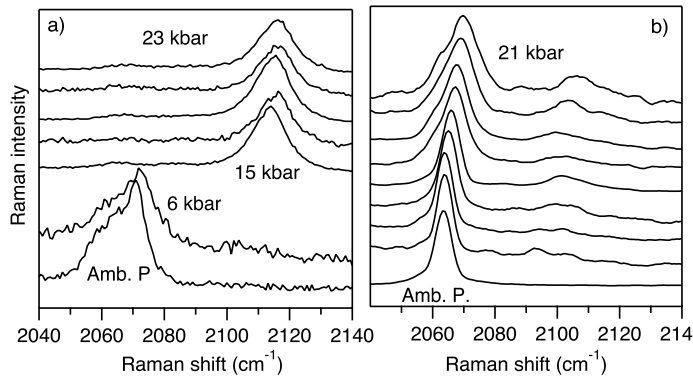


**Fig. 4.** Variable-pressure Raman spectra in the region of the $\nu_{N\text{-}C}$ stretching vibration for *cis*-Fe(1,10-phenanthroline)$_2$(NCS)$_2$, (a) and *trans*-Fe(pyridine)$_4$(NCS)$_2$ (b).

Fig. 4 shows partial Raman spectra of two such compounds, *cis*-Fe(1,10-phenanthroline)$_2$(NCS)$_2$, a thoroughly studied complex with a low-spin form observed at low temperature and high pressure, and *trans*-Fe(pyridine)$_4$(NCS)$_2$, a complex that does not undergo a spin transition at low temperature but for which Raman spectra show evidence for the presence of a minority low-spin form at high pressure.[47] The $\nu_{N\text{-}C}$ stretching mode of the $NCS^-$ ligands is a sensitive probe for this electronic structure change. Its frequency is 2052 $cm^{-1}$ for uncoordinated $NCS^-$ ions, similar to the frequencies of 2063 $cm^{-1}$ and 2069 $cm^{-1}$ for high-spin *trans*-Fe(pyridine)$_4$(NCS)$_2$ and *cis*-Fe(1,10-phenanthroline)$_2$(NCS)$_2$, respectively, at ambient temperature and pressure. The Raman spectra in Fig. 4 show a small frequency increase by approximately +0.2 $cm^{-1}$/kbar for both compounds as pressure increases, a typical behavior for stretching frequencies. At pressures above 1 GPa, a new peak at 2116 $cm^{-1}$ dominates in Fig. 4a, assigned to the $\nu_{N\text{-}C}$ mode of the low-spin form. This change is sudden in the Raman spectra in Fig. 4a, but very gradual in Fig. 4b, which shows the corresponding spectra for *trans*-Fe(pyridine)$_4$(NCS)$_2$, where the peak corresponding to the high-spin frequency persists at all pressures. The $\nu_{N\text{-}C}$ stretching frequency is compared to the N-C bond length in a variety of iron(II) complexes in Fig. 5.

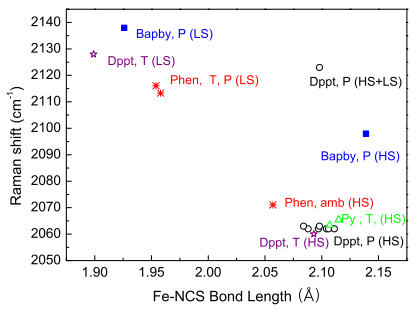


**Fig. 5.** Comparison of the $\nu_{N\text{-}C}$ stretching frequency of $(NCS)^-$ and the Fe-N distance for different iron(II) complexes.

The comparison shows that bond length changes are very small and no quantitative trend can be established for the variation of the frequency as a function of bond length change over this small range, indicating that metal-ligand bonds and other interactions also have a significant effect on the $\nu_{N\text{-}C}$ vibrational frequencies compared in Fig. 5. This overview illustrates that a combination of Raman spectroscopic and structural techniques is useful to understand and guide research on phenomena and properties based on both electronic and structural effects.

## 3 Luminescence of square-planar $d^8$ complexes

Square-planar complexes are particularly attractive for variable-pressure luminescence and structural studies, as both intra- and intermolecular effects can dominate the observed properties. Overviews of the variable-pressure behavior of d-d transitions have been published.[6,7] The typical behavior is illustrated in Fig. 6a for a bis-dithiocarbamato complex of palladium(II).[48] It shows a broad luminescence band characteristic for a d-d transition with a maximum shifting to higher energy by +12 $cm^{-1}$/kbar, in the expected range from +10 $cm^{-1}$/kbar to +30 $cm^{-1}$/kbar. The shift of the maximum is given in the inset at the center of the figure. The comparison with variable-temperature spectra in Fig. 6b is revealing: as temperature increases, the band maximum shifts to lower energy, a trend also shown in the inset. This shift is a consequence of the band broadening on its low-energy side, and indicates an increase of excited-state distortions at higher temperatures. High pressure also prevents the band from broadening on the low-energy side, acting qualitatively similar to low temperature. The comparison in Fig. 6 shows characteristic differences between variable-pressure and variable temperature luminescence due to intramolecular effects including emitting-state properties.

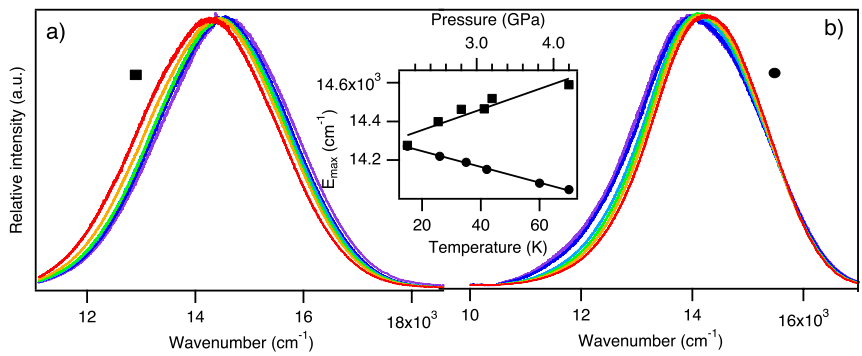


**Fig. 6** (**a**) Pressure-dependent luminescence spectra of $Pd(PDTC)_2$ crystals shown at pressures between 2.1 and 4.2 GPa (red to purple). (**b**) Temperature-dependent luminescence spectra of $Pd(PDTC)_2$ crystals shown at temperatures ranging from 15 to 70 K (red to purple). Inset: variable-pressure luminescence maxima pressure (squares) and variable-temperature luminescence maxima (circles).

An attractive class of complexes for exploring significant pressure-induced structural changes are square-planar complexes with a dangling nucleophile above the coordination plane. Variable-pressure structures for one such compound, $PdCl_2$ (1,4,7-trithiacyclononane) have been published[29] and show a significant pressure-induced decrease of the distance between the dangling nucleophile and the metal

center, a structural change comparable in magnitude to the change in intermolecular distance in Fig. 2. Variable-pressure d-d luminescence spectra of such systems show distinct variations for structurally similar palladium(II) and platinum(II) complexes with identical ligands:[49] a shift to higher energy by +6 $cm^{-1}$/kbar for Pd(1,4,7-trithiacyclononane)$Cl_2$, but to lower energy by -19 $cm^{-1}$/kbar for the platinum(II) analog, a trend qualitatively rationalized by the destabilization of the $d_{z2}$ level in Fig. 3a, labeled intermolecular in the Figure. These shifts are both lower than the typical range given above for d-d transitions, providing experimental evidence for the significant influence of the approaching dangling nucleophile and illustrating that variable-pressure spectra show the trend resulting from the changes to electronic states from all structural modifications. Shifts of band maxima with different signs generally occur because of different electronic effects arising from the small, pressure-induced structural changes. The variable-pressure luminescence spectra therefore show that the effect of the approaching nucleophile is stronger for platinum(II) complexes than for their palladium(II) analogs.

Charge-transfer luminescence transitions for complexes in this class are an appealing next category to explore. Examples are shown in Fig. 7 for representative palladium(II) and platinum(II) complexes with 1,4,7-trithiacyclononane ligands. The observed trends are clearly different from those described above for d-d emissions: no significant shift occurs for the palladium(II) complex and only a small shift to higher energy for the platinum(II) complex. Both bands broaden significantly as pressure increases, indicating strong inhomogeneous broadening. The spectroscopic results suggest that charge-transfer transitions do not react as strongly as d-d bands to structural changes induced by pressure. One possible reason for this difference is that the charge-transfer excited state is ligand-centered and therefore less sensitive to pressure, as strong bonds show only small pressure-induced changes, illustrated by the $\nu_{N\text{-}C}$ stretching frequency and N-C distance in Figs 4 and 5, and only the metal-centered ground state is affected by pressure. In the palladium(II) compound, there appears to be an almost perfect balancing of the effects induced by pressure, leading to no net change of the band maximum, as shown in the inset to Fig. 7. The energy of the charge-transfer luminescence band maximum of the platinum(II) complex increases with pressure, again shown in the inset to Fig. 7, a trend in the opposite direction from the d-d luminescence for platinum(II) complexes with 1,4,7-trithiacyclononane ligands. This difference indicates that the effect of the approaching nucleophile on the $d_{z2}$ level, leading to an energy increase of the ground state and to a decrease of the d-d luminescence energy, is not the dominant effect for this complex. An energy increase of the excited state at higher pressure, likely to occur for the typically $\pi^*$ ligand orbital accepting the metal-centered electron after the excitation, is a probable physical origin of the observed shift. These examples indicate that the electronic structure of the states involved in charge-transfer and d-d transitions do not adapt in the same way to the pressure-induced change of the molecular structure, resulting in different pressure-induced variations.

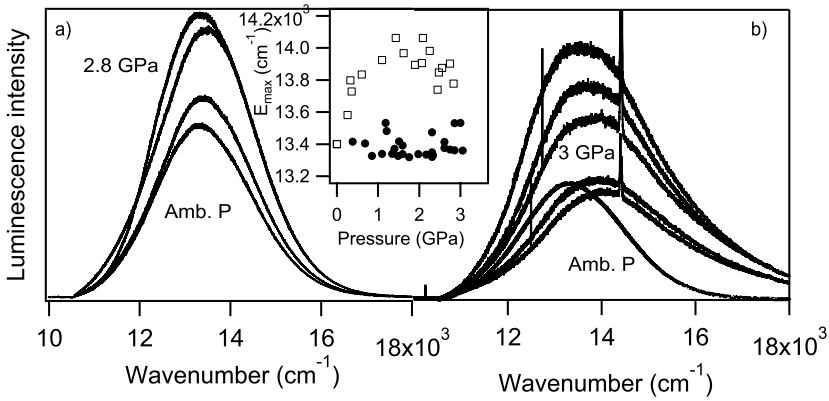


**Fig. 7** Pressure-dependent charge-transfer luminescence spectra of Pd(1,4,7-trithiacyclononane)(phenylpyridine)($PF_6$)·$CH_3CN$ (a), maxima given by solid circles in the inset, and Pt(1,4,7-trithiacyclononane)(5-$NO_2$-phenanthroline)$(PF)_6$ (b)., maxima given as open squares in the inset.

## 4 Aurophilic interactions

Variable-pressure luminescence spectra of dicyanoaurates have been studied in detail as they show dramatic variations of luminescence properties[50] as a consequence of small structural changes, in particular the metal-metal distances. Structures and spectra at variable pressure have been reported, but a correlation is not obvious, as a variety of similar Au(I)-Au(I) distances have to be considered, a challenging situation when several comparable but not identical distances occur.[51] Luminescence spectra show very significant shifts to lower energy on the order of -100 $cm^{-1}$/kbar to -300 $cm^{-1}$/kbar due to the effect of shorter metal-metal distances on the luminescence energy. The schematic view in Fig. 3c qualitatively illustrates the origin of these shifts to lower energy, as the energy of the ground state increases and the emitting-state energy decreases at higher pressure. Dithiocarbamate ligands lead to relatively simple structures, one-dimensional chains with alternating ligand-bridged and unbridged gold(I) centers, a situation closely resembling the schematic view in Fig. 3c.[52] Different substituents of the ligands lead to polymers with almost identical Au(I)-Au(I) distances, but very distinct luminescence properties. Fig. 8 shows variable-pressure luminescence spectra for two such systems, with obvious differences in luminescence band shape and maximum energy, and widely different pressure-induced shifts of the luminescence maxima by -120 $cm^{-1}$/kbar and -40 $cm^{-1}$/kbar. The key reason for this difference by a factor of three is the angular geometry, as schematically indicated by the linear and kinked chains on the right-hand side of Fig. 8, significantly changing the electronic structure of the states involved in the transitions despite the very similar metal-metal distances.[52,53]

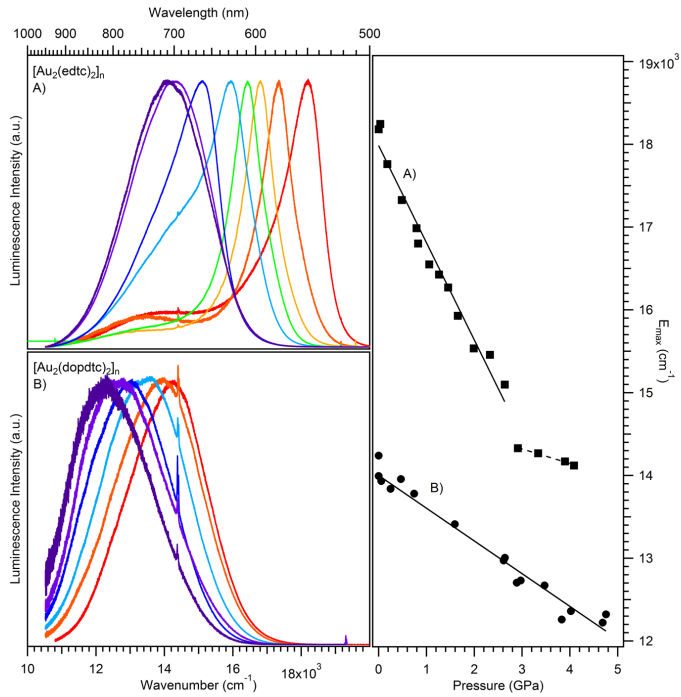


**Fig. 8**.Variable-pressure luminescence spectra and shift of luminescence maxima for two gold(I) dithiocarbamates between ambient pressure and 4.3 GPa.

At pressures above 2 GPa the linear-chain polymer shows broad-band luminescence with a smaller shift, a spectroscopic signature similar to characteristics of the kinked chain and a possible indication of pressure-induced structural defects. This comparison illustrates that pressure-induced structural changes other than distance decreases can have a very important influence on luminescence properties, a very attractive starting point to explore the variable-pressure structures and luminescence spectra of other molecular gold(I) systems in view of applications such as luminescent sensors.

## Conclusion

The preceding overview aims to illustrate the potential of a combined structural-spectroscopic approach based on high-quality data obtained with new-generation instrumentation. Quantitative trends indicate very characteristic differences. This approach is particularly promising for guiding the chemistry of inorganic functional materials, where both the electronic structure of molecular units and their intermolecular interactions have to be understood and controlled in order to optimize materials characteristics.

## References

[a] *Département de chimie, Université de Montréal, Montréal QC H3C 3J7, Canada. E-mail: christian.reber@umontreal.ca*
[b] *Department of Chemistry, University of Cincinnati, Cincinnati OH 45221-0172, USA*
[c] *Departement für Chemie und Biochemie, Universität Bern, CH-3012 Bern, Switzerland*

† The authors thank the Natural Sciences and Engineering Research Council (Canada) for research funding. CR and WBC also thank the Hans and Marlies Zimmer visiting scholar program at the University of Cincinnati for financial support.

1 D. W. H. Rankin, N. Mitzel and C. Morrison, *Structural Methods in Molecular Inorganic Chemistry*, Wiley, 2013.
2 W. Grochala, R. Hoffmann, J. Feng and N. Ashcroft, *Angew. Chem. Int. Ed.*, 2007, **46**, 3620.
3 R. J. Hemley, *Ann. Rev. Phys. Chem.*, 2000, **51**, 763.
4 H. G. Drickamer, *Annu. Rev. Mater. Sci.*, 1990, **20**, 1.
5 H. G. Drickamer and K. L. Bray, *Acc. Chem. Res.*, 1990, **23**, 55-61.
6 C. Reber, J. K. Grey, E. Lanthier and K. A. Frantzen, *Comments on Inorg. Chem.*, 2005, **26**, 233.
7 K. L. Bray, *Top. Curr. Chem.*, 2001, **213**, 1.
8 P. Day, *Angew. Chem. Int. Ed.*, 1980, **19**, 290.
9 P. Day, *Acc. Chem. Res.*, 1988, **21**, 250.
10 J. M. Herrera, P. Franz, R. Podgajny, M. Pilkington, M. Biner, S. Decurtins, H. Stoeckli-Evans, A. Neels, R. Garde, Y. Dromzée, M. Julve, B. Sieclucka, K. Hashimoto, S. Okhoshi and M. Verdaguer, *C. R. Chimie*, 2008, **11**, 1192.
11 R. Bircher, G. Chaboussant, C. Dobe, H. U. Güdel, S. Ochsenbein, A. Sieber and O. Waldmann, *Adv. Funct. Mat.*, 2006, **16**, 209.
12 T. D. Bennett, J. C. Tan, S. A. Moggach, R. Galvelis, C. Mellot-Draznieks, B. A. Reisner, A. Thirumurugan, D. R. Allan and A. K. Cheetham, *Chem.-Eur. J.*, 2010, **16**, 10684.
13 P. Parois, S. A. Moggach, A. R. Lennie, J. E. Warren, E. K. Brechin, M. Murrie and S. Parsons, *Dalton Transactions*, 2010, **39**, 7004.
14 D. Pinkowicz, K. Kurpiewska, K. Lewinski, M. Balanda, M. Mihalik, M. Zentkova and B. Sieklucka, *Crystengcomm*, 2012, **14**, 5224.
15 P. Guionneau, M. Marchivie, Y. Garcia, J. A. K. Howard and D. Chasseau, *Phys. Rev. B*, 2005, **72**, 214408.
16 S. Tancharakorn, F. P. A. Fabbiani, D. R. Allan, K. V. Kamenev and N. Robertson, *J. Am. Chem. Soc.*, 2006, **128**, 9205.
17 A. Prescimone, C. J. Milios, S. Moggach, J. E. Warren, A. R. Lennie, J. Sanchez-Benitez, K. Kamenev, R. Bircher, M. Murrie, S. Parsons and E. K. Brechin, *Angew. Chem. Int. Ed.*, 2008, **47**, 2828.
18 A. Prescimone, C. J. Milios, J. Sanchez-Benitez, K. V. Kamenev, C. Loose, J. Kortus, S. Moggach, M. Murrie, J. E. Warren, A. R. Lennie, S. Parsons and E. K. Brechin, *Dalton Trans.*, 2009, 4858.
19 A. Prescimone, J. Sanchez-Benitez, K. V. Kamenev, J. E. Warren, A. R. Lennie, M. Murrie, S. Parsons and E. K. Brechin, *Z.Naturforsch.(B)*, 2010, **65**, 221.
20 P. Parois, S. A. Moggach, J. Sanchez-Benitez, K. V. Kamenev, A. R. Lennie, J. E. Warren, E. K. Brechin, S. Parsons and M. Murrie, *Chem. Commun.*, 2010, **46**, 1881.

21 T. Granier, B. Gallois, J. Gaultier, J. A. Real and J. Zarembowitch, *Inorg. Chem.*, 1993, **32**, 5305.
22 H. J. Shepherd, S. Bonnet, P. Guionneau, S. Bedoui, G. Garbarino, W. Nicolazzi, A. Bousseksou and G. Molnar, *Phys. Rev. B*, 2011, **84**, 144107.
23 H. J. Shepherd, T. Palamarciuc, P. Rosa, P. Guionneau, G. Molnar, J. F. Letard and A. Bousseksou, *Angew. Chem. Int. Ed.*, 2012, **51**, 3910.
24 C. Slebodnick, J. Zhao, R. Angel, B. E. Hanson, Y. Song, Z. X. Liu and R. J. Hemley, *Inorg. Chem.*, 2004, **43**, 5245.
25 N. Casati, P. Macchi and A. Sironi, *Angew. Chem. Int. Ed.*, 2005, **44**, 7736.
26 G. M. Espallargas, L. Brammer, D. R. Allan, C. R. Pulham, N. Robertson and J. E. Warren, *J. Amer. Chem. Soc.*, 2008, **130**, 9058.
27 N. Casati, P. Macchi and A. Sironi, *Chemistry Eur. J.*, 2009, **15**, 4446.
28 P. J. Byrne, P. J. Richardson, J. Chang, A. F. Kusmartseva, D. R. Allan, A. C. Jones, K. V. Kamenev, P. A. Tasker and S. Parsons, *Chemistry Eur. J.*, 2012, **18**, 7738.
29 D. R. Allan, A. J. Blake, D. G. Huang, T. J. Prior and M. Schroder, *Chem. Commun.*, 2006, 4081.
30 P. Heines, H. L. Keller, M. Armbruster, U. Schwarz and J. Tse, *Inorg. Chem.*, 2006, **45**, 9818.
31 A. Prescimone, J. Sanchez-Benitez, K. K. Kamenev, S. A. Moggach, J. E. Warren, A. R. Lennie, M. Murrie, S. Parsons and E. K. Brechin, *Dalton Transactions*, 2009, **39**, 113.
32 S. A. Moggach, K. W. Galloway, A. R. Lennie, P. Parois, N. Rowantree, E. K. Brechin, J. E. Warren, M. Murrie and S. Parsons, *Crystengcomm*, 2009, **11**, 2601.
33 K. W. Galloway, S. A. Moggach, P. Parois, A. R. Lennie, J. E. Warren, E. K. Brechin, R. D. Peacock, R. Valiente, J. Gonzalez, F. Rodriguez, S. Parsons and M. Murrie, *Crystengcomm*, 2010, **12**, 2516.
34 J. A. Gould, M. J. Rosseinskya and S. A. Moggach, *Dalton Trans.*, 2012, **41**, 5464.
35 E. C. Spencer, N. L. Ross and R. J. Angel, *J. Mat. Chem.*, 2012, **22**, 2074.
36 A. Prescimone, C. Morien, D. Allan, J. A. Schlueter, S. W. Tozer, J. L. Manson, S. Parsons, E. K. Brechin and S. Hill, *Angew. Chem. Int. Ed.*, 2012, **51**, 7490.
37 J. M. Ogborn, I. E. Collings, S. A. Moggach, A. L. Thompson and A. L. Goodwin, *Chem. Sci.*, 2012, **3**, 3011.
38 Y. Okano, B. Zhou, H. Tanaka, T. Adachi, Y. Ohishi, M. Takata, S. Aoyagi, E. Nishibori, M. Sakata, A. Kobayashi and H. Kobayashi, *J. Am. Chem. Soc.*, 2009, **131**, 7169.
39 C. H. Woodall, C. M. Beavers, J. Christensen, L. E. Hatcher, M. Intissar, A. Parlett, S. J. Teat, C. Reber and P. R. Raithby, *Angew. Chem. Int. Ed.*, 2013, **52**, 9691.
40 E. C. Spencer, R. J. Angel, N. L. Ross, B. E. Hanson and J. A. K. Howard, *J. Am. Chem. Soc.*, 2009, **131**, 4022.
41 S. A. Moggach, T. D. Bennett and A. K. Cheetham, *Angew. Chem.-Int. Edit.*, 2009, **48**, 7087-7089.
42 T. D. Bennett, P. Simoncic, S. A. Moggach, F. Gozzo, P. Macchi, D. A. Keen, J. C. Tan and A. K. Cheetham, *Chem. Commun.*, 2011, **47**, 7983.
43 W. Li, M. R. Probert, M. Kosa, T. D. Bennett, A. Thirumurugan, R. P. Burwood, M. Parinello, J. A. K. Howard and A. K. Cheetham, *J. Am. Chem. Soc.*, 2012, **134**, 11940.
44 J. R. Ferraro, *Vibrational spectroscopy at high external pressure: the diamond anvil cell*, Academic Press, New York, 1984.
45 C. M. Edwards and I. S. Butler, *Coord. Chem. Rev.*, 2000, **199**, 1.
46 P. Guionneau, *Dalton Trans.*, 2014, **43**, 382.
47 Y. Suffren, F.-G. Rollet, O. Levasseur-Grenon and C. Reber, *Polyhedron*, 2013, **52**, 1081.

48 C. Genre, G. Levasseur-Theriault and C. Reber, *Can. J. Chem.*, 2009, **87**, 1625.
49 E. Pierce, E. Lanthier, C. Genre, Y. Chumakov, D. Luneau and C. Reber, *Inorg. Chem.*, 2010, **49**, 4901.
50 H. Yersin and U. Riedl., *Inorg. Chem.*, 1995, **34**, 1642.
51 P. Fischer, J. Mesot, B. Lucas, A. Ludi, H. H. Patterson and A. Hewat, *Inorg. Chem.*, 1997, **36**, 2791.
52 F. Baril-Robert, M. A. Radtke and C. Reber, *J. Phys. Chem. C*, 2012, **116**, 2192.
53 R. J. Roberts, N. Bélanger-Desmarais, C. Reber and D. B. Leznoff, *Chem. Commun.*, 2014, **50**, 3148.